Rabi oscillations of Morris-Shore–transformed N-state systems by elliptically polarized ultrafast laser pulses

Hyosub Kim, Yungheung Song, Han-gyeol Lee, and Jaewook Ahn*
Department of Physics, KAIST, Daejeon 305-701, Korea
(Received 4 April 2015; published 26 May 2015)

We present an experimental investigation of ultrafast laser-driven Rabi oscillations of atomic rubidium. Because the broadband spectrum of an ultrafast laser pulse simultaneously couples all of the electronic hyperfine transitions between the excited and ground states, the complex excitation linkages involved with the D_1 or D_2 transition are energy degenerate. By application of the Morris-Shore transformation, this study shows that the considered multistate system is reduced to a set of independent two-state systems and dark states. In experiments performed by ultrafast laser interactions of atomic rubidium in the strong interaction regime, we demonstrate that the ultrafast dynamics of the considered system are governed by no more than two decoupled Rabi oscillations when it interacts with ultrafast laser pulses of any polarization state. We further show the implications of this result with regard to possible control of photoelectron polarizations.

DOI: 10.1103/PhysRevA.91.053421 PACS number(s): 32.80.Qk, 32.80.Wr, 42.65.Re

I. INTRODUCTION

The Morris-Shore (MS) transformation [1] offers a theoretical framework by which the complexity in a variety of coherent excitation coupling linkages of an N-state quantum system can be minimized [2]. Often used in modeling the laser-induced excitation of atoms, the MS transformation replaces the complex system with a decoupled set of independent two-state systems and unlinked states. For example, when a degenerate two-state atom with angular momenta J and J' for the ground and excited levels, respectively, interacts with a laser field, the excitation degeneracy in the magnetic sublevels results in various coupling linkages among $N = 2(J + J' + 1)$ levels, characterized by the polarization states of the laser field. However, a consequence of the MS transformation decoupling is that the $N \times N$ Hamiltonian that describes the coherent excitation is reduced to a set of 2×2 sub-Hamiltonians plus a diagonal matrix that represents uncoupled dark or spectator states. The dynamics of such a system can therefore be described simply by a superposition of independent two-state dynamics, each of which undergoes a Rabi oscillation between a pair of new ground and excited states defined in a factorized Hilbert subspace.

The MS-transformation procedure can be summarized as follows [3]. Suppose that an atomic system with N_1 ground levels and N_2 excited levels ($N = N_1 + N_2$) undergoes a resonant interaction with a laser field. Under the assumption of no damping, the interaction Hamiltonian is written in the rotating-wave approximation (RWA) [4–6] as

$$H = \begin{pmatrix} 0 & V \\ V^\dagger & 0 \end{pmatrix}, \tag{1}$$

where V is an $N_1 \times N_2$ coupling matrix between the ground and excited levels. The MS-transformation theory then predicts that the coupling matrix V is diagonalized by means of an MS transformation given by

$$H' = UHU^\dagger, \tag{2}$$

where the unitary transformation U is defined by

$$U = \begin{pmatrix} X & 0 \\ 0 & Y \end{pmatrix}. \tag{3}$$

Here, the block matrices X and Y are the unitary transformations that diagonalize $VV^\dagger$ and $V^\dagger V$, respectively. The resulting Hamiltonian H' is a direct sum of M sets of two-state systems and $N - 2M$ uncoupled single states ($2M \leqslant \{N_1, N_2\}$), i.e.,

$$H' = \hbar\begin{pmatrix} 0 & \Omega_1 \\ \Omega_1^* & 0 \end{pmatrix} \oplus \begin{pmatrix} 0 & \Omega_2 \\ \Omega_2^* & 0 \end{pmatrix} \oplus \cdots \oplus \begin{pmatrix} 0 & \Omega_M \\ \Omega_M^* & 0 \end{pmatrix} \oplus (h_1) \oplus (h_2) \oplus \cdots \oplus (h_{N-2M}), \tag{4}$$

where Ω_i's are the Rabi frequencies, which are all different in general, of the two-state systems.

Various systems have been analyzed by MS transformation [2], including two-state superposition systems [7,8], three-state Λ-linkage systems [9], four-state diamond- and tripod-linkage systems [10–14], and N-state M- and W-linkage systems [3]. The MS transformation of three-state Λ-linkage systems is of particular interest with regard to the laser technique known as stimulated Raman adiabatic passage (STIRAP) [15], in which the systems undergo an adiabatic evolution between two MS-transformed coupled states, leaving the dark state unpopulated during the laser interaction. The result is a complete population transfer (CPT) [9,16,17] from one ground state to the other, which is easy to understand in the context of the MS transformation.

In this article, we describe an experimental study of MS-transformed N-state systems performed by ultrafast laser-induced coherent excitations. The systems under consideration are the complex coupling linkages of the D_1 and D_2 transitions of atomic rubidium (^{85}Rb). For example, the D_1 transitions from $|5S_{1/2}, F = 2,3\rangle$ to $|5P_{1/2}, F' = 2,3\rangle$ correspond to an $N = 24$ system with $N_1 = 12$ and $N_2 = 12$. We first analyze the atomic rubidium systems in terms of the MS transformation to derive the Rabi frequencies for the D_1 and D_2 transitions induced by an elliptically polarized light in Sec. II. After a brief description of the experimental procedure in Sec. III, our experimental results show that all of the system dynamics

*jwahn@kaist.ac.kr; http://uqol.kaist.ac.kr

are governed by no more than two decoupled Rabi oscillations [18,19] when these systems interact with ultrafast laser pulses of any polarization state. We discuss the implications of this result with regard to the possible control of photoelectron polarization in Sec. IV before giving our conclusions in Sec. V.

II. THEORETICAL CONSIDERATION

A. Linear and circular polarizations

We first consider that a laser pulse in a linear or circular polarization state interacts with the atomic rubidium. Suppose that the polarized electric field is given by

$$\mathbf{E}(t) = \hat{\epsilon}\mathcal{E}(t)\cos(\omega t + \phi), \tag{5}$$

where the polarization vector $\hat{\epsilon} = \hat{z}$ or $(\hat{x} \pm i\hat{y})/\sqrt{2}$ for the linear or circular polarization, respectively. The D_1 transition is dictated by the selection rule of $\Delta m = 0$ or ± 1 ($q = \Delta m$), so for each m, the Hamiltonian can be written in the four-state basis $\{|F = 2,m\rangle, |F = 3,m\rangle, |F' = 2,m \pm q\rangle, |F' = 3,m \pm q\rangle\}$ as

$$H(t) = \begin{pmatrix} 0 & 0 & \mu_{22'}E(t) & \mu_{23'}E(t) \\ 0 & \delta & \mu_{32'}E(t) & \mu_{33'}E(t) \\ \mu^*_{22'}E(t)^* & \mu^*_{32'}E(t)^* & \omega_o & 0 \\ \mu^*_{23'}E(t)^* & \mu^*_{33'}E(t)^* & 0 & \omega_o + \delta' \end{pmatrix}, \tag{6}$$

where $\delta = \omega_{F=3} - \omega_{F=2}$, $\delta' = \omega_{F'=3} - \omega_{F'=2}$, $\omega_o = \omega_{F'=2} - \omega_{F=2}$, and the dipole moments are given by $\mu_{FF'} = \langle F,m|er_q|F',m-q\rangle$.

Because we are considering ultrafast laser interactions, the interaction time is extremely short compared to the inverse of any hyperfine energy splitting, so the effective Hamiltonian under a resonant approximation [20] can be alternatively written in the atomic frame as

$$H(t) = \begin{pmatrix} 0 & 0 & A & B \\ 0 & 0 & C & D \\ A^* & C^* & 0 & 0 \\ B^* & D^* & 0 & 0 \end{pmatrix}, \tag{7}$$

where $A = \mu_{22'}\mathcal{E}(t)/2$, $B = \mu_{23'}\mathcal{E}(t)/2$, $C = \mu_{32'}\mathcal{E}(t)/2$, and $D = \mu_{33'}\mathcal{E}(t)/2$. When $\phi = 0$ is assumed with no loss of generality, the coupling matrix $V(t)$ is given by

$$V(t) = \begin{pmatrix} A & B \\ C & D \end{pmatrix}, \tag{8}$$

and the MS transformation decouples the system into two independent two-state systems through diagonalization of the matrices $V(t)V^\dagger(t)$ and $V^\dagger(t)V(t)$, which are given by

$$V(t)V^\dagger(t) = V^\dagger(t)V(t) = \begin{pmatrix} A^2 + B^2 & AC + BD \\ AC + BD & C^2 + D^2 \end{pmatrix}. \tag{9}$$

The coupling strength of each two-state system, or the square of each Rabi frequency, is then determined by the eigenvalues [2] given by

$$\lambda_\pm = \frac{A^2 + B^2 + C^2 + D^2 \pm \sqrt{(A^2 + B^2 + C^2 + D^2)^2 - 4(AD - BC)^2}}{2}. \tag{10}$$

On the basis of the eigenvectors $|\lambda_\pm\rangle$, an arbitrary ground state can be a pure superposition state or a mixed state of $|\lambda_\pm\rangle$. If these two eigenvalues $\lambda_\pm$ are the same, the two independent oscillators represented by $|\lambda_\pm\rangle$ vibrate coherently with the same Rabi frequency, thus allowing CPT. Here, the condition for $\lambda_+ = \lambda_-$ is given by

$$\{(A + D)^2 + (B - C)^2\}\{(A - D)^2 + (B + C)^2\} = 0. \tag{11}$$

As for the π transitions ($q = 0$), Clebsch-Gordon coefficient symmetries [23] allow $\langle 2m|z|2m'\rangle = -\langle 3m|z|3m'\rangle$ ($A = -D$) and $\langle 2m|z|3m'\rangle = \langle 3m|z|2m'\rangle$ ($B = C$) for all $m = m'$, which satisfies $\lambda_+ = \lambda_-$, and the Rabi frequencies are the same for all m's. Therefore, the entire system undergoes CPT and, moreover, the initial system in any coherent superposition or mixed ground state simply undergoes Rabi oscillation, with the Rabi frequency given by

$$\Omega(t) = \sqrt{\mu^2_{22'} + \mu^2_{23'}}\frac{\mathcal{E}(t)}{2\hbar}. \tag{12}$$

The Rabi oscillations in these complex degenerate-level manifolds have been observed in the implementation of single-qubit operations of atomic rubidium [21].

Meanwhile, the equality $AD = BC$ holds for the σ transitions ($q = \pm 1$), which means that one of the eigenvalues is zero and the other is twice the eigenvalue of $q = 0$ (the π transition). In other words, the σ transitions for different m's have a pair of respective uncoupled states and their Rabi frequencies are $\sqrt{2}$ times larger than those of the corresponding π transitions. Therefore, unlike the π transitions, the temporal dynamics of $\sigma^\pm$ transitions depend on the initial condition because their oscillators are drastically different; this behavior has been applied to coherent controls of medium gains [22].

B. Elliptic polarizations

Now we generalize the problem by considering elliptical polarizations of the laser interaction [3]. When the electric field is defined by

$$\mathbf{E}(t) = \hat{\sigma}_+\mathcal{E}_+(t)\cos(\omega t + \phi_+) + \hat{\sigma}_-\mathcal{E}_-(t)\cos(\omega t + \phi_-), \tag{13}$$

the elements in V are given by $\mathcal{E}_\pm(t)\eta^{m'}_m e^{i\phi_\pm}/2$, where $\eta^{m'}_m$ are the transition dipole moment $\langle Fm|er_{\pm 1}|F'm'\rangle$. The dipole moments can be factorized by a common factor $\mu_{JJ'} = \langle J = 1/2||er||J' = 1/2\rangle$ for all $\{F,m\}$ [23]. When the ellipticity ϵ is defined by $(\mathcal{E}^2_+ - \mathcal{E}^2_-)/(\mathcal{E}^2_+ + \mathcal{E}^2_-)$, the Rabi frequencies are given by

$$\Omega_\pm(\epsilon) = \pm\Omega_o(t)\sqrt{\frac{1 \pm \epsilon}{3}}, \tag{14}$$

with $\Omega_o(t) = \mu_{JJ'}(\mathcal{E}^2_+ + \mathcal{E}^2_-)^{1/2}/2\hbar$.

When the Hamiltonian is MStransformed by means of the summarized procedure in Eqs. (1)–(4), the resulting

Hamiltonian H' is a direct sum of 12 sets of two-state systems given by

$$H' = \hbar\begin{pmatrix} 0 & \Omega_+ e^{i\phi_+} \\ \Omega_+ e^{-i\phi_+} & 0 \end{pmatrix}^{\oplus 6} \oplus \begin{pmatrix} 0 & \Omega_- e^{i\phi_-} \\ \Omega_- e^{-i\phi_-} & 0 \end{pmatrix}^{\oplus 6}, \tag{15}$$

where the first set of six two-state systems corresponds to the σ^+ transitions and the second set corresponds to the σ^- transitions. This result can be readily understood in terms of the basis reduction from $|F,m_F\rangle$ to $|J,m_J\rangle$ [24]. Because spin interactions (in this case, hyperfine interactions) are irrelevant in ultrafast time-scale dynamics, they can be traced out, and the reduced basis description in $|J,m_J\rangle$ can be acquired by alternative means. The advantage of the use of the MS-transformed $|F,m_F\rangle$ bases, instead of the reduced basis set, results from the fact that the coherent dynamics coupled with spin interactions can be directly seen in the former bases, which implies possible applications in ultrafast time-scale nuclear-spin polarization controls [25–27].

III. EXPERIMENTAL PROCEDURE

A schematic of the experimental setup is shown in Fig. 1. The rubidium atoms (^{85}Rb) were cooled and trapped in a conventional magneto-optical trap (MOT) [28]. The details of the experimental setup have been reported elsewhere [21,29,30]. The atoms then interacted with ultrashort laser pulses from a Ti:sapphire mode-locked laser amplifier operating at a pulse repetition rate of 1 kHz. The center wavelength of the laser pulses (the pump pulse) was tuned to 794.7 nm (or 780 nm) for the rubidium D_1 (D_2) transition with a FWHM bandwidth

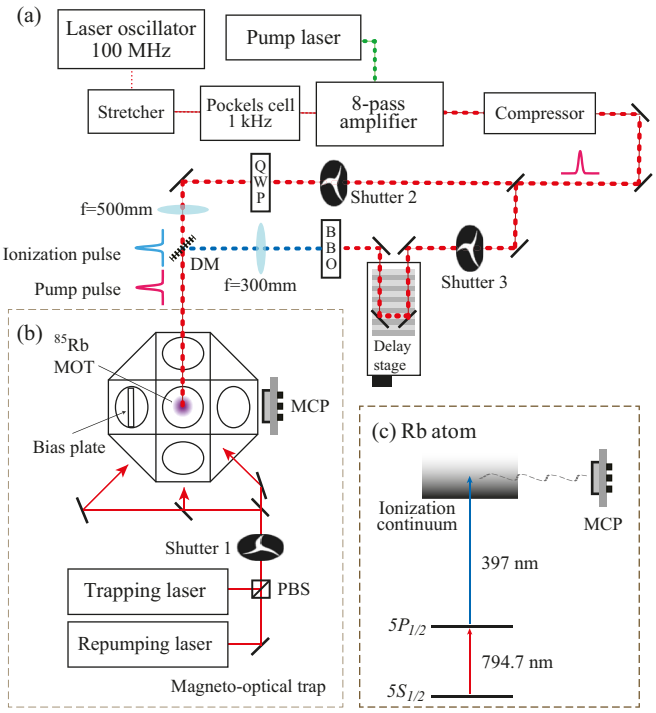

FIG. 1. (Color online) (a) Schematic diagram of the experimental setup. (b) Magneto-optical trapping apparatus for ^{85}Rb. (c) Energy level diagram of ^{85}Rb atoms.

of 3 nm (0.5 nm). The single-pulse energy was varied up to 0.03 mJ, which was equivalent to a Rabi oscillation phase of 2π when the pulse diameter at the atom was about 0.5 mm and the size of the atom cloud was 200 μm. The polarization was controlled by a broadband quarter-wave plate (QWP).

The measurement of the excited state ($5P_{1/2}$ or $5P_{3/2}$) population of the atoms was achieved by photoionization of the excited atoms with frequency-doubled ultrafast pulses (the probe pulse) from the same laser. The pump and probe pulses were independently focused and delivered by a dichroic mirror (DM) to the MOT. The number of ions (Rb^+) was determined with a microchannel plate detector (MCP). The signal linearity was ensured by operating the experiment in the one-photon perturbation regime. The error caused by three-photon ionizations by the pump pulse was estimated to be below 5% at a pulse area of 3π [30], which was negligible in the experimental conditions considered. The entire experiment (four steps: MOT-turn off, laser control, ionization, MOT-turn on) was repeated at 2 Hz by turning three mechanical shutters on and off in a cyclic fashion.

IV. RESULTS AND DISCUSSION

The MS transformation of the rubidium D_1 transitions, described in Sec. II, predicts the following relationship between the accumulated Rabi oscillation phases of the given π and σ transitions:

$$\Theta_\pi = \frac{1}{\sqrt{2}}\Theta_\sigma, \tag{16}$$

which results from Eq. (14) that gives $\Omega_\pm(\epsilon = 0) = \Omega_o/\sqrt{3}$ and $\Omega_\pm(\epsilon = \pm 1) = \pm\sqrt{2/3}\Omega_o$ or zero. In terms of the laser pulse area defined by $\Theta_o = \int \Omega_o(t)dt$, $\Theta_\pi = \Theta_o/\sqrt{3}$, and $\Theta_\sigma = \sqrt{2/3}\Theta_o$. For the same reason, half of the ground levels also remain intact for the σ transitions if the atom is unpolarized, resulting in the relationship of the maximal excitation probabilities given by

$$\mathrm{P}_\pi^{\max} = 2\mathrm{P}_\sigma^{\max}. \tag{17}$$

To verify these predictions, we performed Rabi oscillation experiments with rubidium D_1 transitions by π- and σ-polarized ultrafast laser pulses. The results are shown in Fig. 2, which clearly shows that the Rabi frequency of the σ transition is $\sqrt{2}$ times greater than that of the π transition and that the oscillation amplitude of the σ transition is only half that of the π transition; the two relationships in Eqs. (16) and (17) are thus confirmed. The theoretical calculations are respectively plotted with dashed lines whose deviation from the experimental result is a result of the spatially inhomogeneous laser interaction with the atom ensemble [30]. When the spatial averaging effect is taken into account (by assuming that the size ratio of the Gaussian laser beam and the atom ensemble is 2.5), the new calculations, shown as solid lines, agree well with the experimental results.

Elliptical polarizations are considered in the second experiment. When the rubidium atoms interact with an ultrafast laser pulse in an elliptical polarization, the interaction Hamiltonian in Eq. (7) is expressed as a superposition of the σ^+ and σ^- transitions. In this case, the decoupling is not simply attained by means of a $4\times$ 4 MS transformation $H' = UHU^\dagger$ in

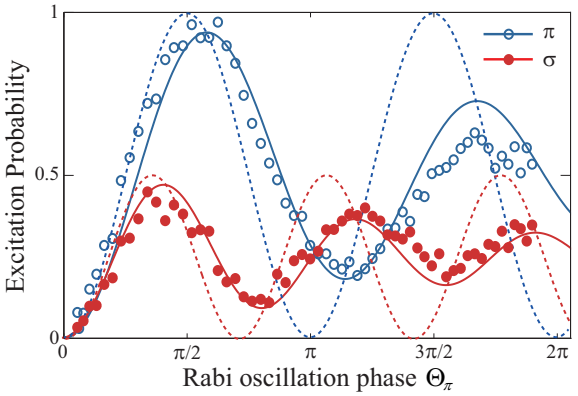

FIG. 2. (Color online) Ultrafast Rabi oscillations of ^{85}Rb atoms between $5S_{1/2}$ and $5P_{1/2}$ energy states. Experimental results for ultrafast laser pulses with linear (π transition) and circular (σ transition) polarization are shown with open blue circles and filled red circles, respectively. Both results are scaled along the vertical axis by the maximal excitation probability of the π transition and along the horizontal axis by the π-transition Rabi oscillation phase (Θ_π). The black dotted lines are the theoretical calculation on the basis of Eq. (18) for the corresponding Rabi oscillations. The new calculations that take into account the spatial average effect are represented by solid lines.

Eq. (3). However, we can still describe the dynamics of the MS-transformed two-state system as a combination of the Rabi oscillations that correspond to the constituent polarization-specific transitions. In the D_1 transitions performed by an elliptically polarized pulse, parts of the two-state system are run by σ^+ and σ^- transitions, respectively. Then, we can decompose the initial ground-state atom, written in $|J,m_J\rangle$ bases, into $|\psi_\pm\rangle$ (the Rabi oscillation bases, respectively, for $\sigma^\pm$ transitions), given by $|\psi_\pm\rangle = a_\pm|1/2, \mp 1/2\rangle$, where $|a_+|^2 + |a_-|^2 = 1$. Therefore, the dynamics of the excited-state population of the atom under an elliptically polarized light pulse predicts the following relationship:

$$\mathrm{P}^{D_1}(\epsilon) = |a_+|^2 \sin^2 \Theta_+ + |a_-|^2 \sin^2 \Theta_-, \qquad (18)$$

where $\Theta_\pm(\epsilon) = \sqrt{(1 \pm \epsilon)/3}\Theta_o$ are the Rabi oscillation phases accumulated by the $\sigma^\pm$ transitions, respectively, from Eq. (15). The π transition is naturally defined for $\epsilon = 0$.

Figure 3 shows the experimental results. The excited state population in $5P_{1/2}$ appears as a degraded oscillation in each ellipticity $\epsilon \in \{0.3, 0.4, 0.45\}$, as shown in Figs. 3(a)–3(c), because, as in Eq. (18), it is given by a sum of two distinct oscillations. The calculation based on Eq. (18) that considers inhomogeneous pulse areas, Θ_o, for various ellipticities is represented in Fig. 3(d). Figure 3(e) shows a closeup of the region around the first peak for various ellipticities. When the ellipticity is changed from zero to one, the first oscillation appears in a gradually smaller Rabi oscillation phase (Θ_π), and the Θ_π for the first peak is changed from π to $\pi/\sqrt{2}$, as shown in Figs. 3(d) and 3(e).

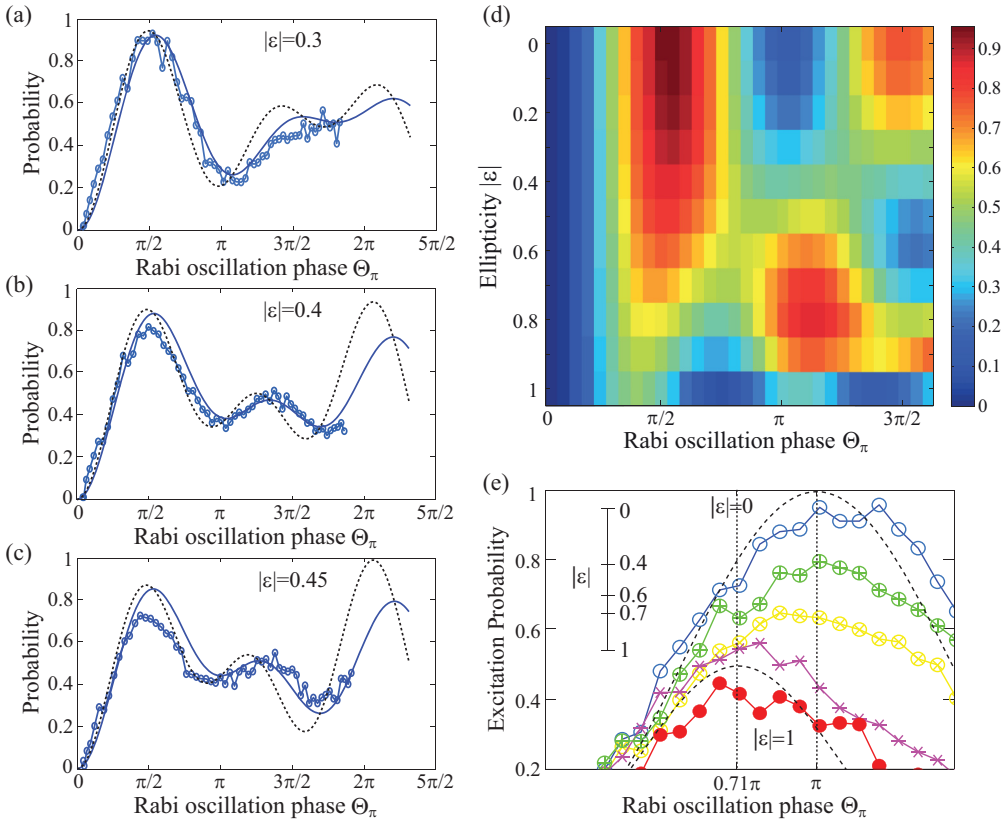

FIG. 3. (Color online) Experimental results (blue circled lines) for D_1 transitions with elliptically polarized lights for (a) $\epsilon = 0.3$, (b) $\epsilon = 0.4$, and (c) $\epsilon = 0.45$. Black dotted lines represent the ideal Rabi oscillation curves, and blue solid lines represent their spatially averaged oscillations. (d) Calculated Rabi oscillations for various ellipticities are represented in a two-dimensional plot. (e) Experimental data for the first peak position are shown close up for various ellipticities.

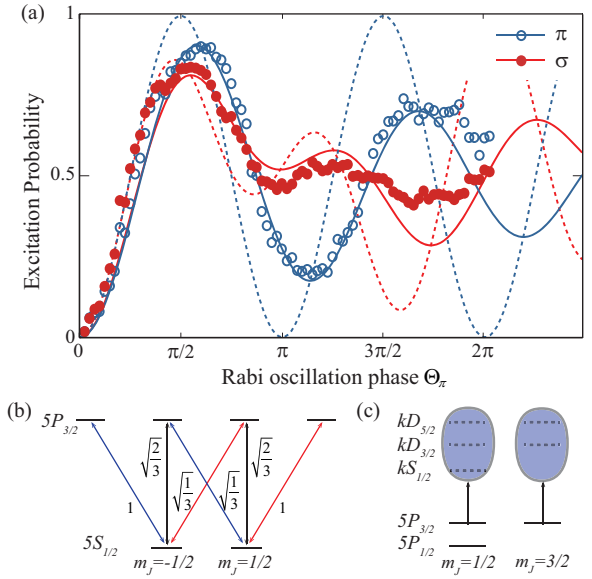

FIG. 4. (Color online) (a) Experimental results for D_2 transitions for circular (blue open circles) and linear (red closed circles) polarization. In comparison, theoretical calculations and their spatially averaged results are represented by dotted and solid lines, respectively. (b) Coupling strengths defined in $|J,m_J\rangle$ bases. (c) Schematic comparison between the ionization schemes for $5P_{1/2}$ and $5P_{3/2}$ states.

Finally, the Rabi oscillations of D_2 transitions between $5S_{1/2}$ and $5P_{3/2}$ energy states are considered. In Fig. 4(a), the experimental results are compared with the theoretical calculations. After a similar argument leading to Eq. (18), the excited state population as a result of D_2 transitions is also given by a sum of two Rabi oscillations as

$$\mathrm{P}^{D_2}(\epsilon) = |a_+|^2 \sin^2 \sqrt{\frac{2+\epsilon}{3}}\Theta_o + |a_-|^2 \sin^2 \sqrt{\frac{2-\epsilon}{3}}\Theta_o, \tag{19}$$

where $\Theta_o^{D_2} = (2\hbar)^{-1}\int_{-\infty}^{t} < 1/2\|er\|3/2\rangle\mathcal{E}(t)dt$ and the $a_\pm$ denote the initial probability amplitudes of the ground state in $|J = 1/2, m_J = \mp 1/2\rangle$ bases. The Clebsch-Gordan coefficients for their coupling to $|J' = 3/2, m'_J\rangle$ bases are shown in Fig. 4(b). However, a direct comparison of the populations of excited atoms in $5P_{3/2}$ levels by counting the photo-ions yields an experimental artifact, because the ionization passages via one-photon transitions to the continuum differ, as shown in Fig. 4(c) for $|J' = 3/2, m'_J = \pm 1/2\rangle$ and $|J' = 3/2, m'_J = \pm 3/2\rangle$. The ratio between the ionization rates may be estimated by comparing the bound-to-bound transitions of the corresponding angular symmetries. Because the coupling strengths from $|J = 3/2, m_J = 1/2\rangle$ and $|J = 3/2, m_J = 3/2\rangle$ are proportional to $\sum_{J'} |\langle 3/2\|ez\|kJ'\rangle < kJ', 1/2|3/2, 1, 1/2, 0\rangle|^2$ and $\sum_{J'} |\langle 3/2\|er\|kJ'\rangle\langle kJ', 3/2|3/2, 1, 3/2, 0\rangle|^2$, respectively, when $|\langle J\|er\|kJ'\rangle|^2 \propto (2J'+1)/(2J+1)$ is assumed, the estimated ratio of the ionization rates is 1.06, which shows good agreement with the value of 1.1 that is used to fit the data to the theoretical calculations in Fig. 4(a).

The remaining experimental errors are the result of laser power fluctuations and the center mismatch between the laser and the atoms, both of which are the predominant deviations in large pulse areas. The laser fluctuation within 10% of the shot-to-shot deviation was maintained at a low level by the event statistics. The size of the atom cloud (200 μm) was small compared to the distance between the steering mirrors (300 mm), so the intrinsic misalignment of 30 μm caused by the steering angular resolution led to an experimental error. However, the guidelines that consider the spatial averaging effect are valid in this experiment [30].

We now turn our attention to the implications of the results obtained in this study to possible applications with regard to the polarization control of electron spins. Electron spin polarization control by photoexcitation of atoms has been theoretically discussed for alkali atoms [31], for which coherent excitations to nP states by circularly polarized light were considered so that spin-orbit coupling exchanged the spin and angular momenta. Alternatively, on the basis of our demonstration, it can be considered that the excited nP state is independently controlled to $nP_{1/2}$ and $nP_{3/2}$ by means of ultrafast Rabi oscillations. Therefore, for example, the procedure to control the electron polarization can be stated as follows. First, a circularly polarized pulse resonantly tuned to $nP_{1/2}$ state completely excites the population in a particular electron spin state, such as the $|m_S = 1/2\rangle$ state, leaving the rest of the spin states intact. The second pulse, which is resonantly tuned to the $nP_{3/2}$ state, then completely excites the remaining ground-state atoms. Finally, the third pulse, which is identical to the first pulse, deexcites the atoms in $nP_{1/2}$ back to their ground state. When the prepared state is photoionized by means of an ultrafast time resolution, the liberated electron will be in a pure spin state. Therefore, with this procedure, ultrafast time-scale electrons of well-defined spin polarizations may be generated.

V. CONCLUSIONS

In summary, we studied the ultrafast laser-driven Rabi oscillations of MS-transformed atomic rubidium transitions. The complex coupling linkages involved with the D_1 or D_2 transitions were analyzed on the basis of the MS transformation, and the simplified decoupled systems were experimentally investigated by ultrafast laser interactions of spatially localized rubidium atoms in a MOT in the strong interaction regime. All of the system dynamics were found to be governed by no more than two decoupled Rabi oscillations for any polarization state of the interacting ultrafast pulse. The implications of this result are discussed with regard to the control of photoelectron polarizations.

ACKNOWLEDGMENTS

This research was supported by Samsung Science and Technology Foundation [SSTF-BA1301-12]. The cold-atom apparatus was constructed in part with support from the Basic Science Research Program [2013R1A2A2A05005187] through the National Research Foundation of Korea.

[1] J. R. Morris and B. W. Shore, Phys. Rev. A **27**, 906 (1983).
[2] B. W. Shore, J. Mod. Opt. **61**, 787 (2013).
[3] N. V. Vitanov, Z. Kis, and B. W. Shore, Phys. Rev. A **68**, 063414 (2003).
[4] L. Allen and J. H. Eberly, *Optical Resonance and Two-Level Atoms* (Dover, New York, 1987).
[5] P. Meystre, *Atom Optics* (Springer-Verlag, New York, 2001).
[6] R. W. Boyd, *Nonlinear Optics* (Academic, Boston, 1992).
[7] N. V. Vitanov, B. W. Shore, R. G. Unanyan, and K. Bergmann, Opt. Commun. **179**, 73 (2000).
[8] N. V. Vitanov, J. Phys. B **33**, 2333 (2000).
[9] N. V. Vitanov, T. Halfmann, B. W. Shore, and K. Bergmann, Annu. Rev. Phys. Chem. **52**, 763 (2001).
[10] J. H. Eberly, B. W. Shore, Z. Bialslashynicka-Birula, and I. Bialslashynicki-Birula, Phys. Rev. A **16**, 2038 (1977).
[11] Z. Bialynicka-Birula, I. Bialynicki-Birula, and J. H. Eberly, and B. W. Shore, Phys. Rev. A **16**, 2048 (1977).
[12] B. W. Shore, Phys. Rev. A **29**, 1578 (1984).
[13] R. G. Unanyan, M. Fleischhauer, B. W. Shore, and K. Bergmann, Opt. Commun. **155**, 144 (1998).
[14] H. Theuer, R. G. Unanyan, C. Habscheid, K. Klein, and K. Bergmann, Opt. Express **4**, 77 (1999).
[15] K. Bergmann, H. Theuer, and B. W. Shore, Rev. Mod. Phys. **70**, 1003 (1998).
[16] W. S. Warren, H. Rabitz, and M. Dahleh, Science **259**, 1581 (1993).
[17] J. S. Melinger, S. R. Gandhi, A. Hariharan, D. Goswami, and W. S. Warren, J. Chem. Phys. **101**, 6439 (1994).
[18] I. I. Rabi, J. R. Zacharias, S. Millman, and P. Kusch, Phys. Rev. **53**, 318 (1938).
[19] I. I. Rabi, Phys. Rev. **51**, 652 (1937).
[20] M. O. Scully and M. S. Zubiary, *Quantum Optics* (Cambridge University, Cambridge, England, 1997).
[21] J. Lim, H.-G. Lee, S. Lee, C.-Y. Park, and J. Ahn, Sci. Rep. **4**, 5867 (2014).
[22] J. C. Delagnes and M. A. Bouchene, Phys. Rev. Lett. **98**, 053602 (2007).
[23] D. M. Brink and G. R. Satchler, *Angular Momentum* (Oxford University, Oxford, 1968).
[24] D. T. Pegg and W. R. Macgillivray, Opt. Commun. **59**, 113 (1986).
[25] T. Nakajima, Phys. Rev. Lett. **99**, 024801 (2007).
[26] M. E. Hayden and E. W. Otten, Phys. Rev. Lett. **101**, 189501 (2008).
[27] T. Nakajima, Phys. Rev. Lett. **101**, 189502 (2008).
[28] W. D. Phillips, Rev. Mod. Phys. **70**, 721 (1998).
[29] S. Lee, H.-g. Lee, J. Cho, J. Lim, C. Y. Park, and J. Ahn, Phys. Rev. A **86**, 045402 (2012).
[30] H.-G. Lee, H. Kim, and J. Ahn, Opt. Lett. **40**, 510 (2015).
[31] M. A. Bouchene, S. Zamith, and B. Girard, J. Phys. B **34**, 1497 (2001).